The Structure and Ferrimagnetic Behavior of *meso*-Tetraphenylporphinatomanganese(III) Tetrachloro-1,4-Benzoquinonide, $[Mn^{III}TPP]^{+}[QCl_4]^{\bullet -} \cdot PhMe$: Evidence of a Quinoidal Structure for $[QCl_4]^{\bullet -}$

Erik J. Brandon, Robin D. Rogers, Brian M. Burkhart, and Joel S. Miller*

Abstract: The redox polymerization of *meso*-tetraphenylporphinatomanganese(II), $Mn^{II}TPP$, and tetrachloro-1,4-benzoquinone, QCl_4, leads to the formation of the magnet *meso*-tetraphenylporphinatomanganese(III) tetrachloro-1,4-benzosemiquinone, $[Mn^{III}TPP]^{+}[QCl_4]^{\bullet -} \cdot PhMe$, which has been characterized by single-crystal X-ray diffraction, magnetic, and thermal measurements. The structure was solved and refined in the monoclinic unit cell, and was found to contain a disordered TPP ligand and toluene solvate, which have conformational parameters restrained to those of other molecules in this series. The disorder, however, does not distract from the overall packing motif. $[Mn^{III}TPP]^{+}[QCl_4]^{\bullet -}$ has a coordination-polymer structure with uniform, one-dimensional linear chains comprising alternating $[Mn^{III}TPP]^{+}$ cations and $[QCl_4]^{\bullet -}$. $[QCl_4]^{\bullet -}$ is μ-*O*-σ-bound to Mn with a Mn–O bond distance of 2.193(4) Å and its structure is reported for the first time. The planar $[QCl_4]^{\bullet -}$ has a quinoid structure. The reduction of QCl_4 to $[QCl_4]^{\bullet -}$ was confirmed by the IR absorption at $\tilde{\nu}_{CO} = 1518\ cm^{-1}$. The Mn-O-C angle is essentially linear while the intrachain Mn···Mn separation is 9.781(2) Å. The magnetic susceptibility between 60 and 160 K can be fit to the Curie–Weiss expression with an effective θ of +32 K. The intrachain antiferromagnetic coupling, J/k_B, is −89 K (−62 cm^{-1}, 134 cal mol^{-1}, 7.5 meV) based on a fitting of the data to the Seiden expression for noninteracting chains comprising alternating quantum ($S = 1/2$) and classical ($S > 1/2$) spins and the Hamiltonian $\mathscr{H} = -2J\boldsymbol{S}_a \cdot \boldsymbol{S}_b$. At 2 and 5 K the saturation magnetization is ≈15800 emuOe mol^{-1}, which is consistent with antiferromagnetic coupling. The a.c. susceptibility indicates two transitions to magnetically ordered states at 13 and at 7 K. The former is frequency-independent and is assigned to a ferrimagnet, while the latter is frequency-dependent and is assigned to a spin glass. At 2 K metamagnetic behavior is observed with a critical field of ≈1.4 kOe. Hysteresis is not observed at 5 K.

Keywords: manganese · magnetic properties · polymers · porphyrinoids · quinones

Introduction

The design and synthesis of magnetically ordered molecular solids continues to focus on new means of attaining a high degree of connectivity between spin-containing moieties.[1, 2] Two classes of molecule-based magnets exist, namely those with active and passive organic ligands. Passive organic ligands position the metal spin sites to modulate the spin coupling, while active organic ligands contribute spins to the magnetic moment in addition to positioning the metal spin sites. Active ligands are rare and have been limited to strong cyanocarbon acceptors, for example, tetracyanoethylene (TCNE) and hexacyanobutadiene, as well as nitronyl nitroxides. Spin-bearing ligands that bond to atoms with a high spin density are expected to exhibit strong spin coupling.[3] In our efforts to obtain new magnetically ordered complexes, we are seeking new active ligands and have examined easily reduced benzoquinones with electron-withdrawing substituents which can act as bridging radical anions. The intrachain coupling should be related to the spin density of the unpaired electron on the atom bound directly to the metal ion.[3] In the case of the *p*-chloranil radical anion, a significant amount of this spin density resides on the oxygen atoms (0.228, based on solid-state ESR measurements of the tetrabutylammonium salt in frozen acetone, and 0.224 from HMO calculations), with lesser amounts residing on the carbon and chlorine atoms.[4]

[*] Prof. J. S. Miller, Dr. E. J. Brandon
Department of Chemistry, 315 S. 1400 E. RM Dock, University of Utah
Salt Lake City, UT 84112-0850 (USA)
Fax: (+1) 801 581 8433
E-mail: jsmiller@chemistry.utah.edu
Prof. R. D. Rogers
Department of Chemistry, The University of Alabama
Tuscaloosa, AL 35487 (USA)
Fax: (+1) 205 348 9104
E-mail: robin@radar.ch.ua.edu
Dr. B. M. Burkhart
Hauptman-Woodward Medical Research Institute
73 High Street, Buffalo, NY 14203 (USA)
Fax: (+1) 716 852 6086
E-mail: burkhart@galen.hwi.buffalo.edu

  0947-6539/98/0410-1938 $ 17.50+.50/0

This is in contrast to the similarly bound $[TCNE]^{\bullet-}$, with a spin density on the nitrogen atoms of 0.13 (from neutron diffraction).[5]

One class of molecule-based magnets are those based upon the redox polymerization of a manganoporphyrin and a strong electron acceptor, for example TCNE in [MnTPP][TCNE] [MnTPP = *meso*-tetraphenylporphinatomanganese(III)]:[6] the $[TCNE]^{\bullet-}$ bridges a pair of hexacoordinate Mn^{III} sites in a *trans*-μ manner. Given this bonding motif we anticipated that the tetrahalogenated benzoquinone acceptors (anils) might form a similar series of magnets and expand the number of active ligands available for the preparation of molecule-based magnets.

Anils have been used to produce charge-transfer salts with, for example, *N*,*N*,*N*′,*N*′-tetramethyl-*p*-diaminobenzene (TMPD),[7a] tetraselenonaphthacene,[7b] and tetrathiafulvalene (TTF),[8] for the preparation of organic conductors. In the last case, alternating chains of $\cdots$DADADA$\cdots$ (D = TTF; A = anil) are present in the solid state. In the TTF–chloranil system, neutral-to-ionic phase transitions have been observed at high pressures.[8b] In this case, conductivity arises from partial charge transfer between the donor and the acceptor, resulting in itinerant conducting electrons. A few 1,4-anil *O*-bound metal complexes have been reported, but none have been structurally characterized.[9]

Although 2,3-dichloro-5,6-dicyanobenzoquinone, DDQ, is a stronger acceptor ($E^o\{[DDQ]^{\circ/-}\} = 0.59$ V; $E^o\{[DDQ]^{2-/-}\} = -0.25$ V vs. SCE),[10] the less sterically encumbered chloranil undergoes a one-electron reduction to form the semiquinone radical anion at $E^o = 0.05$ V and the dianion at $E^o = -0.79$ V in MeCN,[10] which is sufficient to oxidize Mn^{II}TPP. Herein, we report the results of this study including structural and magnetic data.

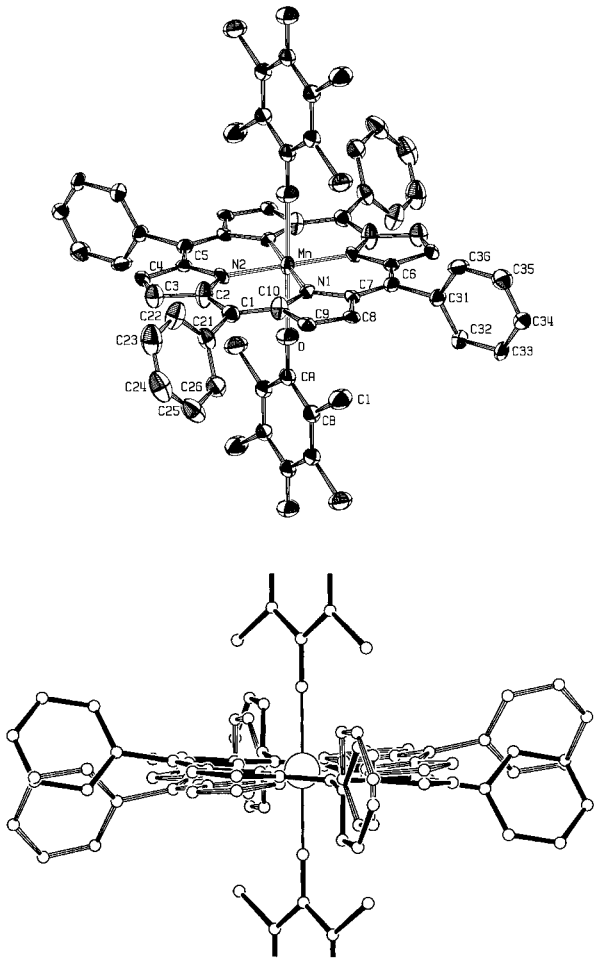

Figure 1. Labeling diagram and ORTEP drawing (50% probability level) for $[Mn^{III}TPP]^+[QCl_4]^{\bullet-} \cdot PhMe$; only one of the two orientations is depicted for clarity. The disordered PhMe is omitted (top), ball-and-stick drawing showing the 9.1° rotational disorder about $C-C6_{symm}$ across the crystallographic mirror plane (bottom).

Results and Discussion

Structure: $[MnTPP]^+[QCl_4]^{\bullet-} \cdot PhMe$ is composed of alternating chains of cations and anions in infinite chains extending along the monoclinic *b* axis. The $[MnTPP]^+$ cations lie on crystallographic inversion centers with Mn^{III} at the center and average $Mn-N_{por}$ distances of 2.010 Å. The deviations of these coordination distances from average are not significant because of the large esds of the atoms in TPP, and they are also consistent with typical $[MnTPP]^+$ distances.[3, 6, 16] The high esds of the TPP atoms arise from an unusual disorder in the TPP ligand: the TPP disorder is a 9.1° rocking across a line joining C6 and $C6_{symm}$ with many atoms, especially those near the $C6-C6_{symm}$ axis nearly superimposed. There is a crystallographic mirror plane midway between these two orientations. The TPP disorder seems to arise from an inefficient filling of the space in the packing of the TPP ligand and the toluene solvate molecules. At the periphery of the TPP the atomic separations are substantial with these phenyl rings exhibiting the greatest C–C separation, Figure 1. Nonetheless, the unrestrained bond distances and angles of the TPP ligand exhibit a stereochemistry similar to other $[Mn^{III}TPP]^+$ cations,[3, 6, 16] but have larger bond esds (≈ 0.01 Å).

Chloranil is completely ordered and is bonded to the Mn^{III} atoms. It sits on a crystallographic inversion center, thus limiting the unique conformational parameters. The C–O, C_O-C_{Cl}, $C_{Cl}-C_{Cl}$, and C–Cl bond distances are 1.253(7), 1.443(5), 1.352(8), and 1.719(4) Å, respectively, which differ from those in QCl_4[12c] by 0.058, −0.044, 0.010, and 0.005 Å, respectively. These increases and decreases are consistent with those expected from the atomic orbital coefficients of the LUMO and indicate a decline in the quinoid character upon reduction to $[QCl_4]^{\bullet-}$. These distances indicate that $[QCl_4]^{\bullet-}$ has a quinoid structure, as observed for both the neutral anil (e. g., QCl_4,[12b] [TTF][QCl_4],[12a] [$Me_2NC_6H_4NMe_2$][QCl_4][7a]) and related reduced anils (e. g., $[DDQ]^{\bullet-}$[13] and [cyanil]$^{\bullet-}$[10, 14]). The quinoid character of the anion coupled with the adjacent chlorine atoms causes the bond angles to differ from an ideal angle of 120°. The ring *ipso* angles around Cl and O are 122° and 115°, respectively. The internal angle between chlorines is also 122°, causing the angle between chlorine and oxygens to decrease to 116°, thereby maintaining planarity. Thus, the shortening of the C–C bond to form the quinoid structures creates steric crowding, which is relieved by the chlorine atoms moving away from each other.

Infrared spectra [and magnetic data (vide infra)] were used to confirm the oxidation state of chloranil. The IR data indicate that QCl_4 has undergone a one-electron reduction, as a significant lowering of the ν_{CO} stretch is observed at 1518 s cm^{-1}. This is comparable to the value of ν_{CO} = 1524 s cm^{-1} reported for $K[QCl_4]$[15] and is substantially lower than the ν_{CO} = 1686 s cm^{-1} reported for QCl_4. The IR spectrum is the same whether the material is synthesized from either benzene or toluene.

There are four disordered components of PhMe at this inversion center, each with an occupancy of 0.25. The electron density in the void space is diffuse; however, the orientations of the toluenes are discernible, so that the toluenes could be restrained to a standard geometry. The disorder is complicated by the presence of two pairs of disordered toluenes with each pair arising from the asymmetric toluene resting on the inversion center and the doubled set arising from an irregular void space created by the disordered TPP ligands. The motion of the TPP ligand is correlated with the toluene disorder. The presence of toluene in the crystal lattice was confirmed by TGA, which revealed a mass loss of $\approx$11% below 225 °C, corresponding to complete desolvation.

The solid-state motif comprises one-dimensional $\cdots D^+A^{\bullet-}D^+A^{\bullet-}\cdots$ chains (D = MnTPP; A = QCl_4), in which the $[QCl_4]^{\bullet-}$ is μ-*O*-σ-bound to Mn with an O – Mn distance of 2.193(4) Å, the Mn-O-C angle is 180.0°, and the dihedral angle between the mean planes of D^+ and $A^{\bullet-}$ is 85.45° (Figure 2). The Mn-O-C angle is larger than the Mn-N-C angles for [MnTPP][TCNE] [148.1(4)°],[6] and [MnTP′P][TCNE] [129(1)°] (H_2TP′P = 3,5-di-*tert*-butyl-4-hydroxyphenyl)porphyrin).[16a] Likewise, the dihedral angle between the mean planes of the porphyrin and $[TCNE]^{\bullet-}$ is substantially greater than the values reported for [MnTPP][TCNE] (69.5°)[6] and [MnTP′P][TCNE] (30.4°),[16a] respectively.

The intrachain Mn ··· Mn separation is 9.781(2) Å, which is 0.33 Å shorter than that reported for [MnTPP][TCNE] and 1.20 Å longer than that observed for [MnTP′P][TCNE].[16a] The interchain in-registry Mn ··· Mn separation for [MnTPP][QCl_4] is 13.133 Å while the out-of-registry Mn ··· Mn separations are 10.523 and 15.243 Å. The interchain separations are 9.317 (out-of-registry), 13.133 (in-registry), and 14.440 Å (out-of-registry).

[MnTPP][QCl_4] has no close contacts between overlapping moieties in the structure, which is comparable to [MnTPP][TCNE][6] and [MnTP′P][TCNE].[16a] The atoms in $[QCl_4]^{\bullet-}$ are in direct van der Waals contact (3.5 Å) with the atoms of the sandwiching phenyl groups from neighboring TPP planes. The disordered phenyl rings fill void spaces and do not appreciably contact any other part of the structure. The closest noncoordinating contact is between the chlorine and C7 of the TPP ring above it. This distance is either 3.24 or 3.42 Å, depending on the rocking state of the TPP ligand, with a mean distance of 3.34 Å. This distance is rather short for a van der Waals contact between carbon and chlorine, which would be expected to have a van der Waals contact of > 4.0 Å. This close contact may be the reason for the disorder of the TPP ligand, although the electron-rich chlorine could be donating some electrons to the electron-deficient TPP ligand in this arrangement.

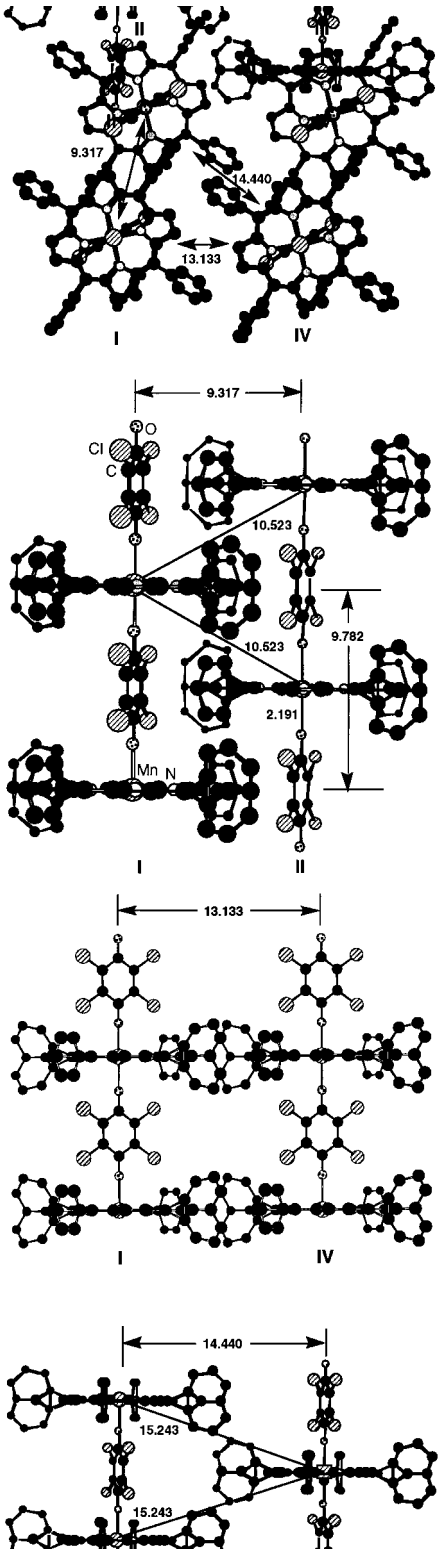

Figure 2. Views of intra- and interchain interaction among the unique chains: I, II, III, and IV for $[Mn^{III}TPP]^+[QCl_4]^{\bullet-}\cdot$PhMe.

0947-6539/98/0410-1940 $ 17.50+.50/0 *Chem. Eur. J.* **1998**, *4*, No. 10

Magnetic behavior: The reciprocal of the corrected molar magnetic susceptibility (χ^{-1}) and moment of [MnTPP][QCl_4], measured at 1000 Oe and 2–300 K, are presented in Figure 3. Above 160 K, the susceptibility can be fit to the Curie–Weiss expression, $\chi \propto 1/(T-\theta)$, with $\theta = 16$, while between 60 and

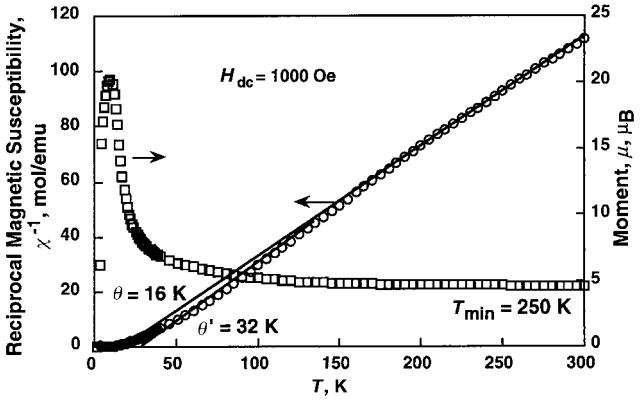

Figure 3. Reciprocal molar magnetic susceptibility, χ^{-1}, and moment, μ, as a function of temperature for polycrystalline $[Mn^{III}TPP]^+[QCl_4]^{\bullet-} \cdot PhMe$.

160 K, the susceptibility can be fit with an effective θ,θ' of 32 K. The latter is in contrast with θ' values of 61 and 90 K reported for uniformly chained [MnTPP][TCNE][6] and [MnTP′P][TCNE],[16a] respectively. The observed room-temperature effective moment, μ_{eff} [$\equiv (8\chi T)^{1/2}$], is 4.63 μ_B, typical for this class of materials,[6, 16a] which increases with decreasing temperature below 250 K until 25 K where it reaches a maximum due to saturation. A minimum characteristic of antiferromagnetic coupling[17] in the $\chi T(T)$ plot, Figure 4, is

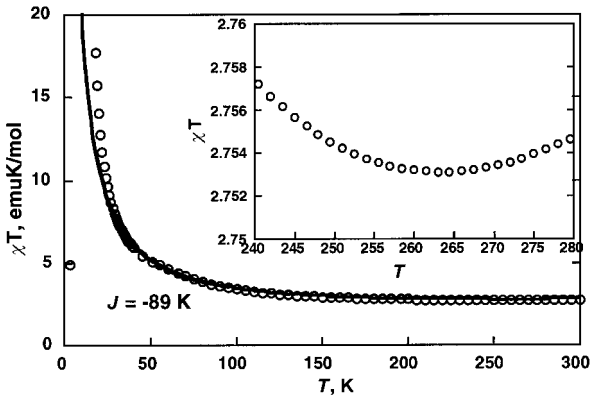

Figure 4. The temperature-dependence of χT and the fit to the Seiden function (solid line).

observed at 260 ± 20 K. The $\chi T(T)$ data can be fit by the Seiden expression[18] for noninteracting chains comprising alternating quantum ($S = 1/2$) and classical ($S > 1/2$) spins using the Hamiltonian $\mathscr{H} = -2J\boldsymbol{S}_i \cdot \boldsymbol{S}_j$ with $J/k_B = -89$ K (-62 cm^{-1}, 134 cal mol^{-1}; 7.5 meV) (k_B = Boltzmann's constant) consistent with ferrimagnetic behavior assuming $g_{Mn^{III}} = 1.985$ and $g_{[QCl_4]^{\bullet-}} = 2.00$. This J reflects the strong intrachain antiferromagnetic coupling. A fit to the Seiden function predicts a broad minimum at 265 K in the $\chi T(T)$ data, which is in agreement with the observed value.

Antiferromagnetic behavior is also evident from the saturation magnetization. The isothermal magnetization at 5 K increases rapidly with the application of a small field, quickly rising to near saturation, M_s (Figure 5). At 5 T, the magnetization is $\approx 15\,800$ emuOe mol^{-1} or 94% of the

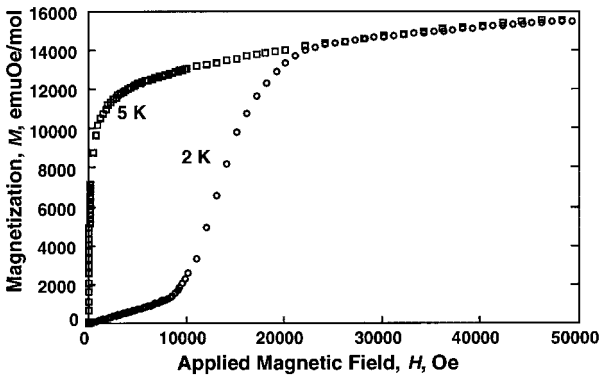

Figure 5. Magnetization as a function of applied magnetic field at 2 and 5 K for polycrystalline $[Mn^{III}TPP]^+[QCl_4]^{\bullet-} \cdot PhMe$.

16 755 emuG mol^{-1} expected for the $\boldsymbol{S}_{Tot} = 2 - 1/2 = 3/2$ system. This is substantially lower than that expected from ferromagnetic coupling, that is, 27 925 emuG mol^{-1} for the $\boldsymbol{S}_{Tot} = 2 + 1/2 = 5/2$ system. At 2 K, metamagnetic behavior is observed (field-induced changeover from an antiferromagnetic ground state to a ferromagnetic ground state) with a critical field of ≈ 1.4 kOe (Figure 5). Similar field-dependent behavior was observed for [MnTPP][TCNE], which exhibits a critical field of ≈ 30 kG at 2.25 K, which corresponds to a spin-flop transition.[19]

In addition to d.c. measurements, the susceptibility was determined in an applied a.c. field of 1000 Oe (< 0.05 d.c. field) at several frequencies and the resulting data are consistent with long-range ferromagnetic order. A peak in the real part of the a.c. susceptibility, χ', is a better indication of T_c (Figure 6). The in-phase component exhibits a sharp frequency-independent increase at ≈ 13 K (accompanied by a peak in χ''), and a frequency-dependent χ' peak centered

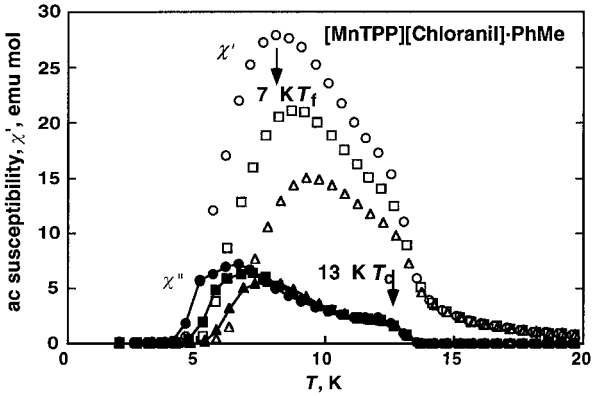

Figure 6. Dispersive, χ', and absorptive, χ'', components of the a.c. susceptibility for $[Mn^{III}TPP]^+[QCl_4]^{\bullet-}$ at 10 (○ and ●, respectively), 100 (□ and ■, respectively), and 997 (△ and ▲, respectively) Hz ($H_{d.c.} < 0.05$ Oe, amplitude = 1000 Oe). The 13 K absorption is frequency-independent, while the lower temperature peak is frequency-dependent. Sample was cooled to zero-field, and data recorded upon warming.

  0947-6539/98/0410-1941 $ 17.50+.25/0

around 7 K (again accompanied by a secondary peak in χ''). The position of these peaks/shoulders, as well as the peak-to-shoulder ratios, are reproducible between samples, which suggests that this behavior is intrinsic to the sample and is not a mixture of two separate phases displaying different magnetic phenomena. The 13 K peak is assigned to a transition to a ferrimagnetic state, while the 7 K peak is assigned to a transition to a spin glass state. These critical temperatures were obtained from the a.c. data measured at 10 Hz. Hysteresis was not observed at 5 K.

Experimental Section

Synthesis: All manipulations were carried out under a nitrogen atmosphere with standard Schlenck techniques or in a Vacuum Atmospheres DriLab under nitrogen. Solvents used were predried and distilled from appropriate drying agents. $Mn^{II}TPP(py)$ (py = pyridine) was prepared by a literature method.[6, 11] Chloranil and QCl_4 (Aldrich) were recrystallized from toluene.

$[MnTPP]^+[QCl_4]^{\cdot-}\cdot PhMe$: Solutions of $Mn^{II}TPP(py)$ (150.7 mg, 0.2018 mmol) in toluene (30 mL) and chloranil (74.7 mg, 0.3038 mmol) in toluene (20 mL) were filtered and then mixed. This mixture was left to stand overnight. The resulting black precipitate was collected, washed three times with fresh, dry toluene (10 mL portions) and dried under vacuum for several hours. Yield: 100.9 mg (50 %); anal. calcd for the monosolvate: $C_{57}H_{36}Cl_4MnN_4O_2$: C 68.08; H 3.60; N 5.57; found: C 67.99; H 3.82; N 5.41; IR (Nujol): $\tilde{\nu}_{CO} = 1518$ (s) cm^{-1}. Single crystals were isolated by means of a similar procedure in which the porphyrin (50.03 mg, 0.0674 mmol) was dissolved in dichloromethane (20 mL) and layered with a solution of chloranil (0.0168 mg, 0.0683 mmol) in toluene (30 mL) by pipette transfer and allowed to stand in a vibration-damped DriLab for several days. A similar procedure was attempted with other halogenated quinones, such as fluoranil, bromanil, iodanil and DDQ, resulting only in the formation of polycrystalline samples.

X-ray structure determination: Isolation of crystals suitable for X-ray diffraction was difficult, and the only crystals obtained were long, thin, shiny, dark red, opaque plates. The crystal was mounted on a fiber, transferred to the goniometer, and flash-frozen to $-100\,^\circ C$ with a stream of cold nitrogen gas. Data was collected at $-100\,^\circ C$ with a Bruker AXS SMART/CCD area detector ($Mo_{K\alpha}$ radiation). Cell constants and an orientation matrix for the data collection were obtained by least-squares refinement of 4763 reflections; a summary of the data collection parameters is given in Table 1. The data was empirically corrected for absorption by means of the program SADABS. Systematic absences and subsequent least-squares refinement were used to determine possible space groups. The initial space group determination revealed either the centric *C*2/*m* or the acentric *C*2 or *Cm*. The crystal structure was solved by direct and difference Fourier methods using SHELXS-97 followed by full-matrix least-squares refinement on F^2. Most of the structure was determined in the centric space group *C*2/*m* with the molecule residing on a 2/*m* site. However, the geometry of the TPP ligand exhibited severe distortion of the phenyl substituents, and a severe bend from the porphyrin plane. Large positive electron density peaks above and below the atoms of the TPP plane suggested that TPP was disordered across the crystallographic mirror plane. We examined larger unit cells exhibiting strong pseudosymmetry as a cause for the disorder; however, the area detection images did not indicate any doubling of cell axes. A satisfactory and chemically reasonable structure was obtained by allowing two distinct occupancies of the TPP moiety related by a 9.1° rotation about an axis joining C6 and $C6_{symm}$. This structure yielded chemically identical phenyl rings across the TPP ring from each other, as in other structures containing TPP, and a relatively planar TPP system. Crystallographic restraints held the toluene atoms in standard geometry. In the final refinement, all nonhydrogen atoms were refined with restrained anisotropic thermal parameters yielding a total of 307 parameters with 377 restraints and $R(F_o)$ of 5.96 % for the 1426 data with $F > 4\sigma(F)$ and 7.80 % for the 1783 total data.

Table 1. Crystallographic details for $[Mn^{III}TPP]^+[QCl_4]^{\cdot-}\cdot PhMe$.

chemical formula	$C_{57}H_{36}Cl_4MnN_4O_2$
M_r, daltons	1005.70
space group	*C*2/*m*
a	18.655(2) Å
b	9.781(2) Å
c	13.133(2) Å
β	102.028(2)°
V	2343.9(5) $Å^3$
Z	2
T	$-100\,^\circ C$
λ	0.710730 Å
ρ_{calcd}	1.424 $g\,cm^{-3}$
μ_{calcd}	0.56 mm^{-1}
$R(F_o)$[a]	0.0596
$R(F_o)$[b]	0.0780
$R_w(F_o^2)$[c]	0.1541

[a] $\Sigma\,||F_o|-|F_c||/\Sigma\,|F_o|$ for $F > 4\sigma(F)$. [b] $\Sigma\,||F_o|-|F_c||/\Sigma\,|F_o|$ for $F > 0\sigma(F)$. [c] $\{\Sigma[w(F_o^2-F_c^2)^2]/\Sigma[w(F_o^2)^2]\}^{1/2}$ and $w = 1/\sigma^2(F_o^2)+(0.08P)^2+8.9P$ and $P = [\max(F_o^2, 0)+2F_c^2]/3$.

Physical methods: The magnetic susceptibility was determined at 2 – 300 K on a Quantum Design MPMS-5XL5T SQUID magnetometer (sensitivity = 10^{-8} emu or 10^{-12} emu Oe^{-1} at 1 T) in an ultra-low field ($\approx$ 0.005 Oe), and a.c. options by means of a reciprocating sample measurement system, and continuous low-temperature control with enhanced thermometry features. The a.c. magnetic susceptibility (χ' and χ'') was studied in the range of 1 mHz to 1 kHz. Samples were loaded in an airtight Delrin® holder and packed with oven-dried quartz wool (to prevent movement of the sample in the holder). For isofield measurements, the samples were cooled to zero-field (by following the oscillation of the d.c. field), and data was collected upon warming. For d.c. isothermal and a.c. measurements, remanent fluxes were minimized by oscillation of the d.c. field, followed by quenching of the magnet. Remaining fluxes were detected by means of a flux gate gaussmeter and further minimized by the application of an opposing field, to bring the d.c. field to <0.5 Oe. The diamagnetic correction of -608.5×10^{-6} emu mol^{-1} was used for $[MnTPP]^+[QCl_4]^{\cdot-}\cdot PhMe$.

The thermal properties were studied on a TA Instruments Model 2050 thermal gravimetric analyzer (TGA) (ambient to 1000 °C) located in a Vacuum Atmospheres DriLab under nitrogen to protect air- and moisture-sensitive samples. Samples were placed in an aluminum pan and heated at 20 °C min^{-1} under a continuous flow of nitrogen (10 mL min^{-1}). The infrared spectra ($\nu = 625-4000$ cm^{-1}) were obtained on a Perkin – Elmer 783 spectrophotometer and on a Mattson Galaxy Series FTIR 3000 spectrophotometer. Elemental analyses were performed by Atlantic Microlabs, Norcross, GA (USA).

X-ray crystal structure analysis: Crystallographic data (excluding structure factors) for the structure reported in this paper have been deposited with the Cambridge Crystallographic Data Centre as supplementary publication no. CCDC-101 035. Copies of the data can be obtained free of charge on application to CCDC, 12 Union Road, Cambridge CB2 1EZ, UK (fax: (+44) 1223-336-033; e-mail: deposit@ccdc.cam.ac.uk).

Acknowledgments: The authors appreciate the constructive comments and insight provided by Prof. E. Coronado (Universidad de Valencia), Prof. A. J. Epstein, Dr. C. M. Wynn, and M. Girtu (The Ohio State University), and gratefully acknowledge support from the U.S. Department of Energy Division of Materials Science (Grant No. DE-FG03-93ER45504) and the National Science Foundation (Grant No. CHE9320478).

Received: January 28, 1998 [F980]

[1] Proceedings of the conference on *Ferromagnetic and High-Spin Molecular Based Materials* (Eds.: J. S. Miller, D. A. Dougherty), *Mol. Cryst. Liq. Cryst.* **1989**, *176*; Proceedings of the conference on *Molecular Magnetic Materials* (Eds.: O. Kahn, D. Gatteschi, J. S. Miller, F. Palacio), *NATO ARW Molecular Magnetic Materials*, **1991**, *E198*; Proceedings of the conference on the *Chemistry and Physics of*

  0947-6539/98/0410-1942 $ 17.50+.50/0

Molecular-Based Magnetic Materials (Eds.: H. Iwamura, J. S. Miller), *Mol. Cryst. Liq. Cryst.* **1993**, *232/233*; Proceedings of the conference on *Molecule-Based Magnets* (Eds.: J. S. Miller, A. J. Epstein), *Mol. Cryst. Liq. Cryst.* **1995**, *271–274*; Proceedings of the conference on *Molecular-Based Magnets* (Eds.: K. Itoh, J. S. Miller, T. Takui), *Mol. Cryst. Liq. Cryst.* **1997**, *305/306* (Eds.: M. M. Turnbull, T. Sugimoto, L. K. Thompson), *ACS Symp. Ser.* **1996**, *644.*

[2] Reviews: a) A. L. Buchachenko, *Russ. Chem. Rev.* **1990**, *59*, 307, *Usp. Khim.* **1990**, *59*, 529; O. Kahn, *Molecular Magnetism*, VCH, **1993**; b) A. Caneschi, D. Gatteschi, R. Sessoli, P. Rey, *Acc. Chem. Res.* **1989**, *22*, 392; D. Gatteschi, *Adv. Mater.* **1994**, *6,* 635; c) J. S. Miller, A. J. Epstein, W. M. Reiff, *Acc. Chem. Res.* **1988**, *21*, 114; J. S. Miller, A. J. Epstein, W. M. Reiff, *Science* **1988**, *240*, 40; J. S. Miller, A. J. Epstein, W. M. Reiff, *Chem. Rev.* **1988**, *88*, 201; J. S. Miller, A. J. Epstein, *New Aspects of Organic Chemistry* (Eds.: Z. Yoshida, T. Shiba, Y. Ohsiro), VCH, New York, NY **1989**, *237*; J. S. Miller, A. J. Epstein, *Angew. Chem.* **1994**, *106,* 399; *Angew. Chem. Int. Ed. Engl.* **1994**, *33,* 385; J. S. Miller, A. J. Epstein, *Adv. Chem. Ser.* **1995**, *245*, 161; J. S. Miller, A. J. Epstein, *Chem. Eng. News* **1995**, *73* (#40), 30.

[3] K-i. Sugiura, A. Arif, J. Schweizer, L. Öhrstrom, A. J. Epstein, J. S. Miller, *Chem. Eur. J.* **1997**, *3*, 138.

[4] M. Broze, Z. Luz, B. L. Silver, *J. Chem. Phys.* **1967**, *46*, 4891; E. Melamud, B. L. Silver, *J. Phys. Chem.* **1974**, *78*, 2140; A. Bieber, J. J. Andre, *Chem. Phys.* **1974**, *5*, 166; B. S. Prabhananda, C. C. Felix, J. S. Hyde, A. Walvekar, *J. Chem. Phys.* **1985**, *83*, 6121.

[5] A. Zheludev, A. Grand, E. Ressouche, J. Schweizer, B. Morin, A. J. Epstein, D. A. Dixon, J. S. Miller, *J. Am. Chem. Soc.* **1994**, *116,* 7243.

[6] J. S. Miller, J. C. Calabrese, R. S. McLean, A. J. Epstein, *Adv. Mater.* **1992**, *4*, 498.

[7] a) J. L. de Boer, A. Vos, *Acta Crystallogr.* **1968**, *B24,* 720; b) A. Onodera, I. Shirotani, H. Inokuchi, N. Kawai, *Chem. Phys. Lett.* **1974**, *25*, 296.

[8] a) J. B. Torrance, A. Girlando, J. J. Mayerlee, J. I. Crowley, V. W. Lee, S. J. LaPlaca, *Phys. Rev. Lett.* **1981**, *47*, 1747; b) B. Toudic, M. H. Lemee-Cailleau, J. Gallier, H. Cailleau, F. Moussa, *Phase Trans.* **1991**, *32*, 241.

[9] S. L. Kessel, D. N. Hendrickson, *Inorg. Chem.* **1978**, *17*, 2630; S. L. Kessel, D. N. Hendrickson, *Inorg. Chem.* **1980**, *19*, 1883; E. Uhlig, *Z. Chem.* **1989**, *9*, 305; E. Balough-Hergovich, G. Spier, *Inorg. Chim. Acta* **1988**, *147*, 51; A. Vleck, A. A. Vleck, *Inorg. Chim. Acta* **1983**, *69*, 191; S. Kobayashi, S. Iwata, M. Abe, S-i. Shoda, *J. Am. Chem. Soc.* **1990**, *112*, 1625.

[10] C. Vazquez, J. C. Calabrese, J. S. Miller, D. A. Dixon, *J. Org. Chem.* **1993**, *58*, 65.

[11] L. R. Milgrom, *Tetrahedron* **1983**, *39*, 3895.

[12] a) J. J. Mayerle, J. B. Torrance, J. I. Crowly, *Acta Crystallogr.* **1979**, *B35*, 2988; b) S. S. C. Chu, G. A. Jeffrey, T. Sakurai, *Acta Crystallogr.* **1962**, *15*, 661.

[13] J. S. Miller, D. A. Dixon, *Science* **1987**, *235*, 871.

[14] The structure of $Li^+[QCl_4]^{\bullet-}$ has also been reported; however, bond distances are unreliable owing to poor resolution: M. Konno, H. Kobashai, F. Marumoo, Y. Saito, *Bull. Chem. Soc. Jpn.* **1973**, *46*, 1987.

[15] Y. Iida, *Bull. Chem. Soc. Jpn.* **1970**, *43*, 345.

[16] See, for example: a) A. Böhm, C. Vazquez, R. S. McLean, J. C. Calabrese, S. E. Kalm, J. L. Manson, A. J. Epstein, J. S. Miller, *Inorg. Chem.* **1996**, *35,* 3083; b) J. T. Landrum, K. Hatano, W. R. Scheidt, C. A. Reed, *J. Am. Chem. Soc.* **1980**, *102*, 6729; C. L. Hill, M. M. Williamson, *Inorg. Chem.* **1985**, *24*, 2834, 3024; E. B. Fleischer, *Acc. Chem Res.* **1970**, *3*, 105; W. R. Scheidt, C. A. Reed, *Chem. Rev.* **1981**, *81*, 543; P. Turner, M. J. Gunter, T. W. Hambley, A. H. White, B. W. Skelton, *Inorg. Chem.* **1992**, *31*, 2297.

[17] E. Coronado, M. Drillon, R. Georges, in *Research Frontiers in Magnetochemistry* (Ed.: C. J. O'Connor), World Scientific, **1993**, 26; D. Beltran, E. Coronado, M. Drillon, R. Georges, *Stud. Inorg. Chem.* **1983**, *3*, 589; E. Coronado, M. Drillon, D. Beltran, R. Georges, *Chem. Phys.* **1983**, *79*, 449; M. Verdaguer, M. Julve, A. Michalowicz, O. Kahn, *Inorg. Chem.* **1983**, *22*, 2624; M. Drillon, J. C. Gianduzzo, R. Georges, *Phys. Lett. A*, **1983**, *96A*, 413.

[18] J. Seiden, *J. Phys. Lett.* **1983**, *44,* L947.

[19] P. Zhou, B. G. Morin, A. J. Epstein, R. S. McLean, J. S. Miller, *J. Appl. Phys.* **1993**, *73*, 6569.

  0947-6539/98/0410-1943 $ 17.50+.25/0